Electronic Polarization Reversal and Excited State Intramolecular Charge Transfer in Donor/Acceptor Ethynylpyrenes

Shu-Wen Yang,[†] Arumugasamy Elangovan,[†] Kuo-Chu Hwang,[‡] and Tong-Ing Ho*[,†]

Department of Chemistry, National Taiwan University, Taipei 106, Taiwan, and Department of Chemistry, National Tsing Hua University, Hsin Chu 300, Taiwan

Received: April 22, 2005; In Final Form: July 6, 2005

An attempt to tune the electronic properties of pyrene (Py) by coupling it with a strong electron donor (−$PhNMe_2$, DMA)/acceptor (anthronitrile, AN) through an ethynyl bridge has been undertaken. A moderate electron donor (^{i}PrOPh−, IPP)/acceptor (2-quinolinyl, 2Q) has also been incorporated, and all four molecules were studied with reference to a neutral molecule, namely, 1-phenylethynylpyrene (PhEPy). All the arylethynylpyrenes (ArEPy's) have been thoroughly characterized, and their electronic properties were studied by absorption and emission spectral properties of these ArEPy's. The electrochemical characteristics were also studied for arriving at the electrochemical band gap which has been compared with the HOMO−LUMO energy gap derived from the photophysical measurements and theoretical calculations performed by density functional theory (DFT) using B3LYP/6-31G* basis sets. The results obtained from experimental and theoretical studies are critically discussed.

Introduction

Pyrene (Py) is one of the most widely studied fluorophore. Its durable electronic properties[1] and its supramolecular chemistry have been put to use, by introducing appropriate structural modifications, in many applications that include, among others, the development of sensors[2] and molecular photonic devices.[3]

Intramolecular charge transfer (ICT) in organic systems have been widely investigated in order to understand the factors controlling the charge separation and charge recombination.[4] Electronic interaction and charge transfer efficiencies in donor−acceptor systems based on pyrene (as acceptor) have been recently studied with experimental and theoretical results, and these probes have the donors directly linked to the pyrene fluorophore through a C−C σ-bond or through conjugation via phenylene rings.[5]

It has been well established that organic π-conjugated donor−acceptor (D−A) molecules have potential applications in electronics such as electrooptic devices,[6] light-emitting diodes,[7] and field effect transistors.[8] Our synthetic ability, coupled with accessibility to a wealth of fabrication techniques, makes it possible to realize smart materials for our future needs. The Sonogashira coupling approach has been proved to be one of the best established techniques for the synthesis of a wide variety of ethynyl conjugated organic materials.[9]

Charge recombination of electrolytically generated radical ions in solutions leads to the formation of electronically excited states of molecules by energetic electron transfer reactions at the electrified interface. Such excited species emit energy in the form of fluorescence. This process is called electrogenerated chemiluminescence or electrochemiluminescence (ECL).[10] ECL emission is believed to occur via one of three different routes: directly from singlet excited state (S-route), via triplet−triplet annihilation (T-route), or via excimer formation (E-route).[11] Excimers[12] are homodimers that exist in the excited state of molecules in solution. Many excimers are formed between molecules whose π-systems interact effectively leading to the formation of appropriate states, and they possess structures prominently governed by their monomer chemical structures. The formation of excited states in the solid state by application of electric field (as in OLED) has been shown to follow a mechanism similar to that in solution (ECL).[13] Hence the study of electronic properties of more new donor−acceptor molecular systems is necessary to gain a better understanding of the basis underlying the electron transfer processes occurring in materials upon interaction with external stimuli such as electromagnetic radiation and addition and removal of electrons to and from the molecules.

To the best of our knowledge, pyrene linked to either electron donors or electron acceptors through a C−C triple bond has not been studied yet. As a further extension of our research[14] on the design and development of new electronic materials (electro- and photoactive organic molecules), we have designed here a set of molecules based on pyrene that is linked to donors and acceptors via an ethynyl bridge.

In the present work the compounds shown in Chart 1 were synthesized and studied for their electronic properties with the idea of tuning them by appropriate choices of donors and acceptors linked to the pyrene chromophore via a ethynyl linkage. Strong and weak electron donors were coupled to the pyrene, and their charge transfer properties were compared with those of strong and weak electron acceptor linked pyrenes having a control molecule, namely, phenylethynylpyrene (PhEPy).

Results and Discussion

Chart 1 depicts the chemical structures of the compounds studied in the present work. All the arylethynylpyrene (ArEPy) compounds were prepared by the coupling reaction of the corresponding terminal arylacetylenes with 1-bromopyrene under Sonogashira conditions. A summary of the photophysical

* Corresponding author. Fax: +886-2-23636359. E-mail: hall@ntu.edu.tw.
[†] National Taiwan University.
[‡] National Tsing Hua University.

10.1021/jp052086u CCC: $30.25
Published on Web 08/12/2005

CHART 1: Chemical Structures of Arylethynylpyrene Compounds Studied in the Present Work: *N,N*-Dimethylanilinoethynylpyrene (DMAEPy), 4-Isopropoxyphenylethynylpyrene (IPPEPy), Phenylethynylpyrene (PhEPy), 2-Quinolinylethynylpyrene (2QEPy), and 9-Anthronitrilo-10-ethynylpyrene (ANEPy)

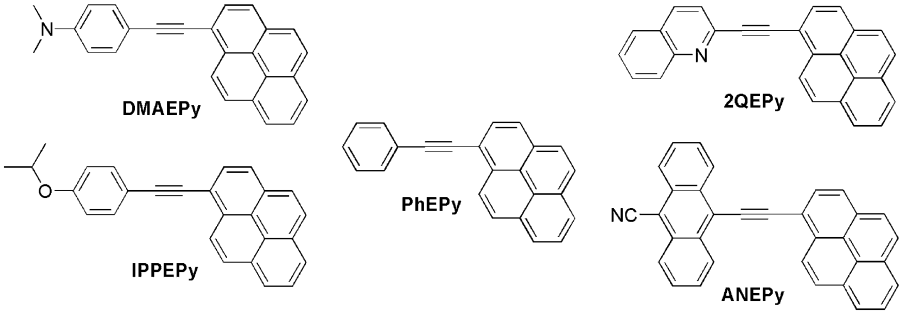

TABLE 1: Photophysical Data of Arylethynylpyrenes (ArEPy's) in Acetonitrile (10^{-5} M)

compd	λ_{max}^{abs} (nm)	ΔE_{H-L}[a] (eV)	ϵ_{max}[b]	λ_{max}^{fl} (nm)	Φ[c]	τ_{fl}[d] (ns)
DMAEPy	388	2.76	3.11	540	0.83	3.47
IPPEPy	386	3.18	2.17	480	0.98	1.98
PhEPy	381	3.14	4.45	392	1.00	4.85
2QEPy	395	2.99	3.88	444	0.83	2.05
ANEPy[e]	472	2.48	1.80	556	0.45	4.60

[a] HOMO−LUMO gap calculated from the onset of the UV−visible absorption maxima. [b] In $\times 10^5$ M^{-1} cm^{-1}. [c] Using coumarin 1 standard ($\Phi = 0.5$ in MeOH).[15] [d] Fluorescence lifetime measured in aerated MeCN excited at λ_{max} (see Supporting Information for profiles). [e] $c = 10^{-6}$ M.

TABLE 2: Electrochemical Data and ECL Spectral Maxima for ArEPy's Recorded in Acetonitrile with 50 mM TBAP at a Scan Rate of 50/s

compd	concn[a]	$E_{p,Ox}$ (V)	$E_{p,Red}$ (V)	ΔE_{H-L}[b] (eV)	$-\Delta H°$ [c] (eV)	λ_{max}^{ECL} (nm, eV)
DMAEPy	1.0 mM	0.92	−0.92	1.84	1.68	510, 2.431
IPPEPy	0.5 mM	1.33	−0.90	2.23	2.07	509, 2.436
PhEPy	1.0 mM	1.41	−0.92	2.23	2.17	
2QEPy	0.5 mM	1.18	−1.11	2.29	2.13	
ANEPy	saturated	0.91	−0.83	1.74	1.58	

[a] Different concentrations were chose due to varying solubility for each compound. [b] HOMO−LUMO gap calculated as the difference between the two peak potentials. [b] Calculated using the equation $\Delta H° = E_{p,Ox} - E_{p,Red} - 0.16$.[10k]

data of these compounds is presented in Table 1, and the electrochemical characteristics are furnished in Table 2.

Photophysical Properties. The photophysical characteristics of the ArEPy's are given in Table 1. The UV−vis absorption spectra of the compounds recorded in acetonitrile clearly display the effect of substitution on Py. Figure 1a depicts the electronic absorption spectra of ArEPy's in which we can see that PhEPy shows an absorption pattern very similar to that of pyrene (or 1-methylpyrene),[5b] but with the longer wavelength band shifting to the red due to the extension of π-conjugation. IPPEPy (bearing a weak electron donor) and 2QEPy (bearing a weak electron acceptor) show further red shifts with a slight loss of vibronic structure indicating moderate charge transfer. The strong electron donor substituted DMAEPy and the strong electron acceptor substituted ANEPy show more pronounced shifts to the red with the DMA pushing the absorption tail well into the visible region and AN doing so strongly that the longer wavelength band is seen at about 475 nm. The corresponding shorter wavelength band usually appearing at about 275 nm for free pyrene (or 1-methylpyrene) appears red shifted by more than 20 nm for the majority of the compounds and by over 100 nm for AN-substituted ethynylpyrene.

While all molecules show lower energy bands as compared to free pyrene (or 1-methylpyrene) due to the extension of conjugation, they all show only very mild charge transfer absorption spectra. However, the fluorescence emission spectra (Figure 1b) of the compounds recoded in the same solvent clearly display the nature of the emitting state possessing charge transfer character. The spectra apparently lose the characteristic pyrenyl fluorescence emission. Both electron acceptors and electron donors effectively induce charge transfer in the excited state which can be seen from the continual appearance of lower energy bands upon increasing both the donor strength and acceptor strength relative to the neutral PhEPy, which shows a secondary vibronic shoulder band. In all, the shift to the longer wavelength region spans more than 150 nm. Among these compounds the strongest donor substituted and strongest acceptor substituted molecules, namely DMAEPy and ANEPy, show the most red-shifted emission. The pyrene behaves as an electron acceptor in the former while it behaves as a donor in the latter.

The fluorescence lifetime in acetonitrile as obtained by time-correlated single photon counting measurements revealed that the τ_{fl} is higher for strong acceptor substituted ANEPy and for strong donor substituted DMAEPy. Neither the weaker donor nor the weaker acceptor had higher lifetimes, and in fact both IPPEPy and 2QEPy have almost the same excited-state lifetimes. The excited state of PhEPy, having a neutral structure, shows a lifetime of ~5 ns. It may be noted that all these molecules have ~1% of the excited-state lifetime of the free pyrene (~308 ns/MeCN). The results were reproducible within 10% variation in either the absence or presence of oxygen in the solution. Since all the lifetimes are quite short, whether the solutions were degassed did not make a difference in the lifetime values in view of the slower diffusion rate of oxygen compared with the lifetime. The shorter lifetime for the excited states of these molecules should be the result of efficient charge transfer in these systems.

This kind of intramolecular charge transfer can be better understood by performing solvatochromic studies, and we have carried out the same for all compounds in various solvents of different polarity. The fluorescence emission spectra of ArEPy's recorded in the various solvents are shown in Figure 2. PhEPy (center) has been found to experience no charge transfer (CT) in the excited state as seen from the maintenance of the vibronic structure of the emission band in all solvents. Only a slight (<10 nm) red shift in the emission maxima was noticed for this molecule. However, very strong ICT is discernible for strong donor and strong acceptor substituted DMAEPy and ANEPy. The weaker donor and weaker acceptor substituted IPPEPy and 2QEPy display milder ICT as seen from the gradual loss of fine structure from less polar hexane through medium polar

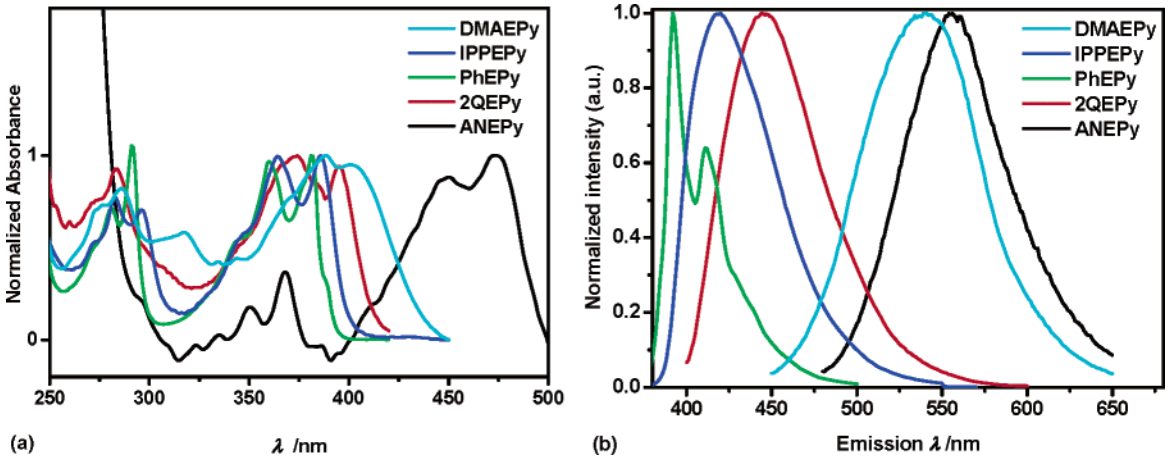

Figure 1. UV−visible absorption spectra (a) and fluorescence emission spectra (b) of arylethynylpyrenes in CH_3CN.

tetrahydrofuran (THF) down to high polar dimethyl sulfoxide (DMSO).

The vast red shift observed in the strong donor and strong acceptor substituted ethynylpyrenes is interesting in that the structured band of DMAEPy appears in hexane at 475 nm while the same band for ANEPY appears at 480 nm, indicating that the excited states of both of these compounds have very nearly the same energy levels. The shift observed for these two molecules did not vary much as the largest shift observed for both compounds in DMSO appears similar (550 nm for DMAEPy and 560 nm for ANEPy).

A fluorophore is considered to be a dipole because of its bipolar structure. This dipole (with dipole moment μ) in solution can interact with its surrounding medium characterized by its dielectric constant (ϵ) and refractive index (n). The interaction produces changes in energy of both the ground state and excited state of the molecule. As a result, the fluorophore emits light of different energy, and the difference between the ground state and excited state energy levels is given as Stokes shift. This Stokes shift is a property of the solvent refractive index and dielectric constant. The influence of local molecular environment on the optical property of the molecules studied here can be understood by using the Lippert equation, a model that describes the interactions between the solvent and the dipole moment of chromophore.[16]

$$\nu_{abs} - \nu_{fl} = (2/hc)[\Delta f]\{(\mu^* - \mu)^2/a^3\} + \text{constant}$$

where

$$\Delta f = [(\epsilon - 1)/(2\epsilon + 1)] - [(n^2 - 1)/(2n^2 + 1)]$$

and a is the radius of the chromophore.

Plots of solvent polarity (or the orientation polarizability, Δf) against the Stokes shift in various solvents are linear for most compounds studied (see the Supporting Information). The best correlation is observed for stronger electron donating substituent (DMAEPy) (Figure 3) and AnEPy where reversed electronic polarization is observed. For systems with weak electron donor−acceptor (PhEPy), the correlation is not as good. Better correlations can be obtained by plots without dioxane solvent for an unknown reason. We have also tried correlations using the Kamlet−Taft solvent polarity parameter α, β, and π^*.[24] The simplified Kamlet−Taft equation applied to sovatochromic shifts is given in eq 1.

$$\upsilon_{max} = \upsilon_0 + a\alpha + b\beta + s(\pi^* + d\delta) \qquad (1)$$

where υ is the value for the wavenumber of indicated fluorescence maximum and υ_0 is the value for the reference solvent (cyclohexane). α is the HBD (hydrogen bond donating) ability, β is the HBA (hydrogen bond accepting) ability, and π^* is the dipolarity/polarizability of the solvent. δ is a polarizability correction term that is zero for nonchlorinated aliphatic solvents. a, b, s, and d are solvent-independent coefficients. The coefficient of d is zero for all electronic spectra that shift bathochromically with increasing solvent polarity. b is zero for aprotic compounds. In our experiment, a non-HBD solvent ($\alpha = 0$) is chosen, and acetonitrile and methylene chloride are excluded since $\alpha \neq 0$. Thus, the solvent effect on υ_{max} depends only on π^*. There is a better result in the Kamlet−Taft plot compared to that in the Lippert−Mataga correlation (see Figure 3 and the Supporting Information).

Concentration quenching experiments were also conducted for selected compounds, and we found that increasing the concentration of the solute molecules produces excimer emission bands located about 75 nm to the red of the original emission maxima for PhEPy with a concomitant decrease in the emission intensity. DMAEPy and IPPEPy did not show excimer bands (see the Supporting Information).

Electrochemistry. Cyclic voltammograms (CVs) were recorded to determine the electrochemical activity and to arrive at the reduction and oxidation potential values of these compounds. CVs were recorded in acetonitrile with 50 mM tetrabutylammonium perchlorate (TBAP) as supporting electrolyte at a scan rate of 0.05 V/s. The reduction and oxidation peak potentials are recorded in Table 2.

The one-electron oxidation for PhEPy occurs at a value very similar to that of 1-ethynylpyrene ($E_{p,Ox} = -1.47$ V vs Ag/Ag^+); however, the reduction reaction occurs at a much lower value than for either pyrene or 1-ethynylpyrene.[17] The oxidation and reduction peak potentials for all the compounds are very much affected by the substituents in that both the strong donor (DMAEPy) and the strong acceptor (ANEPy) bring down the oxidation potential to a much greater degree than the weaker donor (IPPEPy) and weaker acceptor (2QEPy). The electrochemically derived HOMO−LUMO gap (ΔE_{H-L}) has been found to be the smallest for the strong donor and strong acceptor substituted compounds. The annihilation enthalpy change ($-\Delta H°$) values and the ECL data are collected in Table 2 and are discussed under the Electrochemiluminescence section (see below).

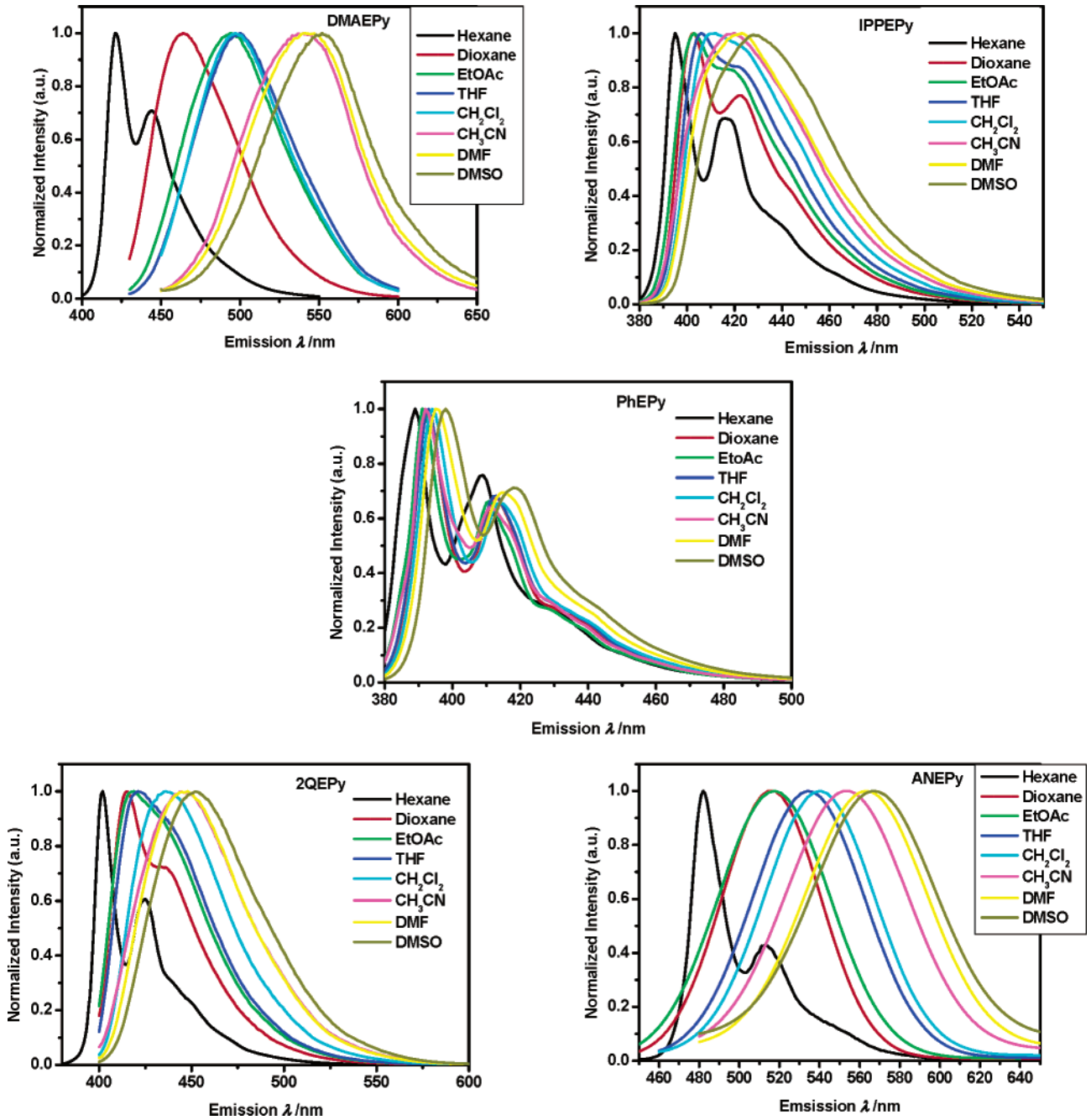

Figure 2. Fluorescence solvatochromic spectra of ArEPy's recorded in various solvents of differing polarity (10^{-5} M).

Computations

We carried out density functional theoretical (DFT) calculations to get a better understanding of the geometric and electronic structure of the molecules presented in this study. We sought that the observation of the electronic properties could also be supported by analyzing the results obtained from density functional calculations carried out using Becke's three-parameter set with Lee−Yang−Parr modification (B3LYP) with 6-31G* basis set of theory. The calculated highest occupied molecular orbital (HOMO) and the lowest unoccupied molecular orbital (LUMO) surfaces of the molecules along with their electrostatic potential maps in the ground states are furnished in Figure 4.

The geometry of these molecules (all in the gas phase) is interesting: the strong donor and the strong acceptor make the resultant molecules remain twisted while weak donor and weak acceptor make the molecules remain planar. The neutral PhEPy, however, remains twisted, too. However, the dipole moment and the dipole vectors change with varying the donor and acceptor. Accordingly, strong donor and strong acceptor cause a greater dipole in the whole molecule and weak donor and weak acceptor cause only a moderate dipole moment change, with that of neutral PhEPy remaining slightly larger than that of pyrene (μ = 0.0 D). The dipole moment vector, which remains pointed within the pyrenyl moiety for the neutral PhEPy, turns slowly toward the direction of pyrene when stronger donors are introduced, and it changes direction toward electron-withdrawing substituents when stronger acceptors are introduced, indicating reversal of polarization.

The HOMO of the DMAEPy remains localized on the donor DMA group and the LUMO on the acceptor pyrene moiety. The situation is reversed in the case of ANEPy, in which the HOMO is found fully localized on the pyrene moiety while the LUMO is found on the AN moiety, also indicating reversal of

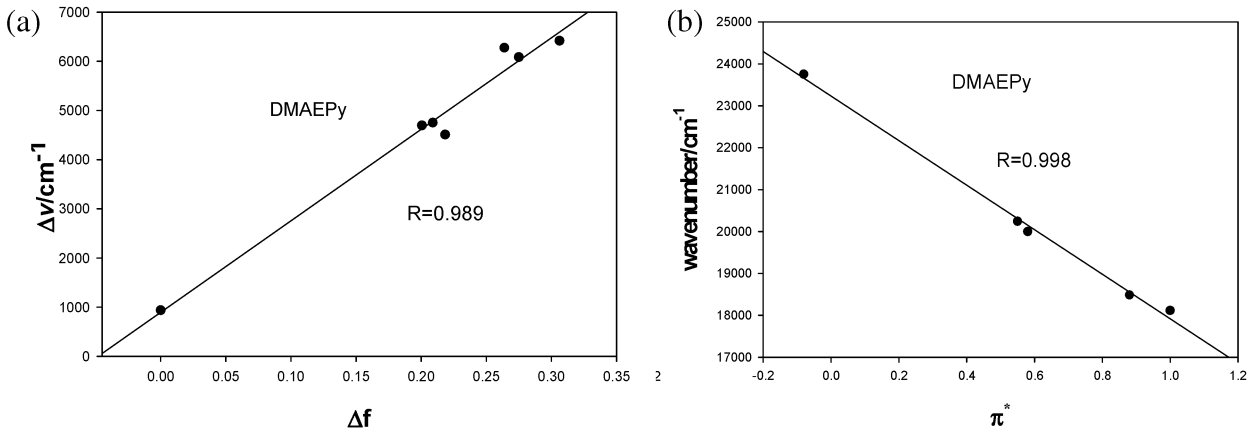

Figure 3. (a) Correlation of orientation polarization (Δf) of solvent media with Stokes shift ($\Delta \nu$) for DMAEPy. (b) Correlation of wavenumber of fluorescence with Kamlet−Taft solvent parameter (π^*) for DMAEPy.

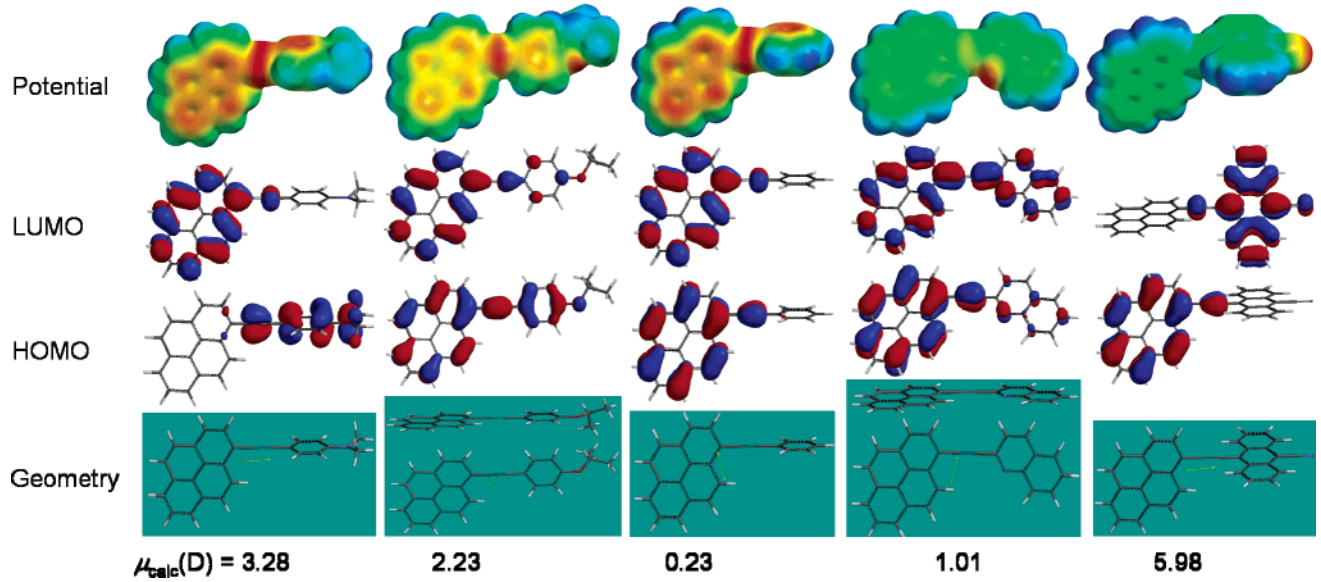

Figure 4. DFT calculated ground-state geometries (with dipole vectors), HOMO, LUMO, and potential energy surfaces (from bottom to top) of ArEPy's.

orbital structures and eventual polarization shift. The localization of HOMO and LUMO on either side of the ethynyl linkage (with contribution from the ethyne to both HOMO and LUMO) suggests that the ethyne acts as a conjugation bridge in all the molecules and CT transition during electronic excitation is effective. As a result, we observe excellent ICT in DMA- and AN-substituted ethynylpyrene molecules. The weak donor IPP-substituted and weak acceptor 2Q-substituted ethynylpyrenes have planar geometry. Their HOMOs and LUMOs are very likely to appear spread all over the molecules, but the actual molecular orbital surfaces indicate that the IPPEPy has its major LUMO coefficient on the pyrenyl moiety and 2QEPy has its HOMO on the pyrenyl moiety (the reverse case scenario). The electrostatic potential maps indicate drifting of charges from the pyrene to the anthronitrile moiety in ANEPy and toward pyrene from the donor moiety in DMAEPy.

The energy levels of the HOMO and LUMO of these molecules (Figure 5) show that the strong donors cause an increase of both energy levels and the stronger acceptor coupled to the pyrene decreases the energy levels relative to neutral PhEPy.

The energy gaps, values in electronvolts (eV), obtained from the theoretical calculations and UV−visible absorption maxima and electrochemical data are depicted in Figure 6. Apart from

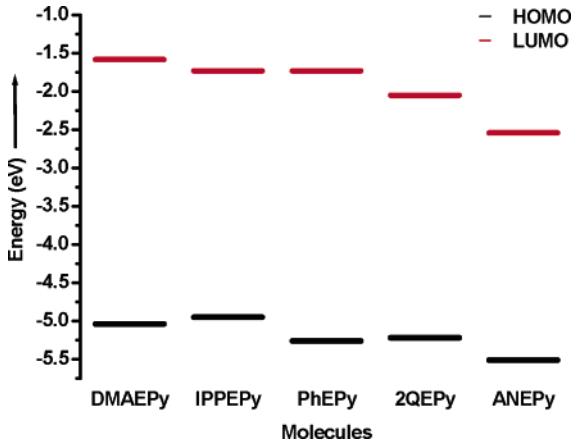

Figure 5. HOMO−LUMO energy levels of ArEPY's. This energy level diagram shows the influence of the donor substituents on the HOMO and LUMO energies.

a slight variation for each compound, there is a satisfactory correlation of the data from theory and UV−vis absorption maxima in that all compounds show a similar trend except the DMA-substituted molecule. While the observed electronic properties of all compounds can be well explained by the orbital coefficients obtained from the DFT calculations, the HOMO−

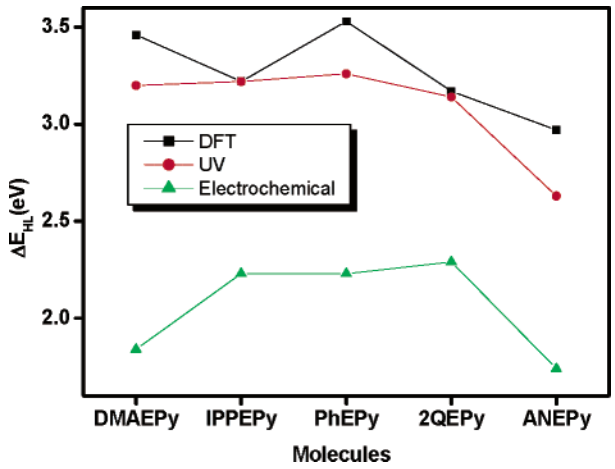

Figure 6. Comparison of experimental [optical (UV−vis λ_{max}/eV) and electrochemical] energy gaps with theoretical values.

LUMO gap as obtained from the DFT results and electrochemical results appear to differ vastly.

The electrochemical data in Table 2 also derive support from the theoretical calculations. The one-electron oxidation can occur from the HOMO and the one-electron reduction on the LUMO of the molecules. Thus, on comparing the data in Table 2 and the HOMO and LUMO surfaces in Figure 4, it is clear that the oxidation process of all but DMAEPy occurs on the pyrene moiety whose π-conjugation has been extended by ethynyl linkage. DMAEPy has the HOMO on the donor moiety and the LUMO on the acceptor moiety with both orbital coefficients extending to the ethyne bridge. Further, the IPP donor and 2Q acceptor have minor contributions to the LUMO. As a result, the redox process can be expected to be unique for these two molecules, unlike DMAEPy and ANEPy. This has been found to be the case in Table 2.

Electrochemiluminescence. ECL spectra were recorded in acetonitrile at 1.0 and 0.10 mM concentrations with 50 mM tetrabutylammonium perchlorate as supporting electrolyte in a cell setup similar to the previously published one.[18] The electrodes were pulsed between the first oxidation and first reduction peak potentials at various pulse intervals to generate radical ions and induce annihilation reaction. Satisfactory ECL spectra were obtained at 10^{-3} M concentration of sample solution, while no ECL was observed at lower or higher concentrations. A saturated solution was necessary for ANEPy because of its poor solubility. However, only the donor substituted DMAEPy and IPPEPy showed ECL emission, while the rest did not show ECL under various conditions of measurements.

The ECL maximum (Table 2 and Figure 7) for DMAPy is found blue shifted relative to the photoluminescence of the compound in the same solvent. However, the IPPEPy shows red-shifted ECL. The observation of blue-shifted ECL can be explained on the basis of *H*-excimer formation in view of efficient π-interaction between the proximally parallel molecules that get closer during the formation of an encounter complex under annihilation reaction condition and in view of its twisted geometry enabling alignment of pyrene heads stacked face to face with donor tail groups projecting away.[19] The red shift for weak donor IPPEPy can be explained as the excimer emission in view of both π-stacking interaction under the above condition and in view of its planar structure. The ECL emission can be considered as arising from a state generated after triplet−triplet annihilation[25] in view of insufficient energy of annihilation as detemined form their $-\Delta H$ values (higher than ECL emission maxima in electronvolts).

Conclusion

Electronic polarization and electronic properties of pyrene have been reversed by coupling electron-donating and electron-withdrawing moieties through ethynyl conjugation. Five different molecules were synthesized with varying degrees of donor and acceptor strengths relative to a neutral molecule, namely phenylethynylpyrene. The absorption and emission spectra reveal that the electronic properties are affected by the extension of π-conjugation via an ethynyl bridge and incorporation of donors and acceptors. Strong donor (dimethylanilino) substituted ethynylpyrene and strong acceptor (9-anthronitrile) substituted ethynylpyrene show excellent intramolecular charge transfer in the excited state while showing no charge transfer in the ground state. The effect of π-extension has been noticed from the shifting of absorption maxima to the lower energy region. The ICT character of all the compounds has been analyzed by solvaotchromic spectral studies that reveal the effect of substitutions. The electrochemical redox potentials of these molecules suggest strong influence of donor and acceptor moieties relative to the neutral phenylethynylpyrene. Only two compounds (DMAEPy and IPPEPy) emit electrogenerated chemiluminescence (ECL). Compounds without a donor moiety and those having electron acceptor moieties do not emit ECL. Observation of ECL from only DMAEPy and IPPEPy and not from other compounds in this series suggests that a donor group is required to generate an excited state that can emit light. The ECL for DMAEPy is blue shifted with respect to its photoluminescence, adding support to our claim that ECL compounds capable of undergoing $\pi-\pi$ interaction having strong donor moieties produce *H*-excimer ECL and those having weaker donors produce usual excimer ECL.[19]

Experimental Section

Materials and Methods. Dichlorobis(triphenylphosphine)-palladium(II) was prepared either in house or from a commercial source, and tetrakis(triphenylphosphine)palladium(0) was from a commercial source (Aldrich). Solvents were distilled as per the standard methods and purged with argon before use. Triethylamine (TEA) and tetrahydrofuran (THF) were distilled and purged with a mixture of approximately 1:1 argon and hydrogen before use. ^{1}H NMR spectra of the samples were recorded with a Varian 400 MHz instrument and ^{13}C NMR spectra were recorded with the same instrument at 100.1 MHz operator frequency in $CDCl_3$ solvent with $CHCl_3$ internal standard (δ 7.24 ppm for ^{1}H and 77 ppm, middle of the three peaks, for ^{13}C spectra). Mass spectra were recorded on nitrobenzyl alcohol matrix. Thin-layer chromatography (TLC) was run on Merck precoated aluminum plates (Si 60 F_{254}). Column chromatography was run on silica gel (60−120 mesh) and neutral alumina (70−230 mesh). All UV−visible spectra were recorded on a HITACHI U-3010 spectrophotometer with 10 μM solution of the compounds, and all fluorescence spectra were recorded on a HITACHI F-4500 fluorescence spectrophotometer using similar solution concentrations in various solvents. Quantum yields were determined using coumarin 1 as standard ($\Phi = 0.5$ in MeOH).[16,18] The fluorescence lifetime measurements were carried out using a single photon counter, Model OB 900, Edinburgh, UK. The solvent was acetonitrile with or without degassing. The concentration was 5 mM for all compounds throughout.

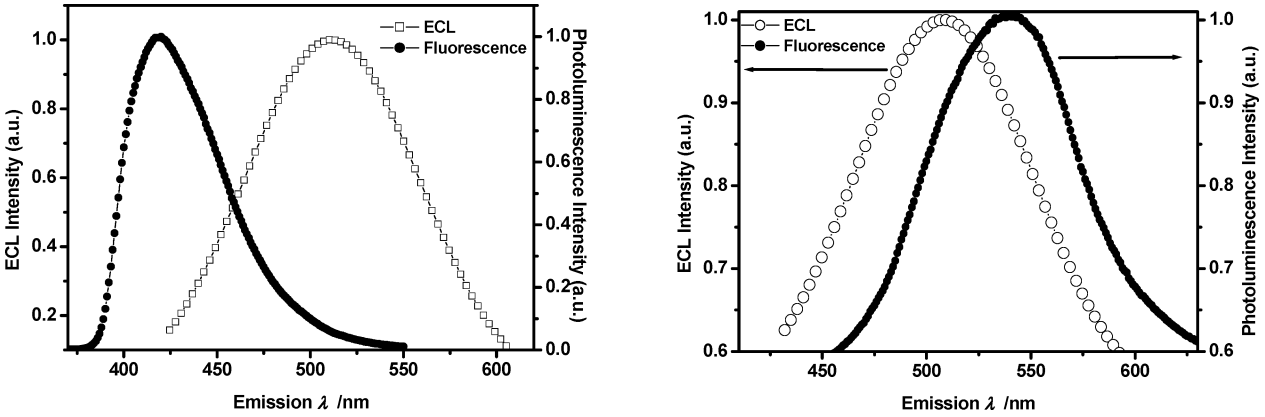

Figure 7. Comparative fluorescence and ECL spectra of IPPEPy (left) and DMAEPy (right) recorded in acetonitrile (10^{-3} M) containing TBAP supporting electrolyte (50 mM).

CV measurements were done on a CH Instruments electrochemical analyzer for solutions of the compounds in deaerated acetonitrile with a scan rate of 50 mV/s. The cell used was a three-electrode cell consisting of a carbon disk (2.0 mm) working electrode, a platinum wire counter electrode, and an Ag/AgCl reference electrode. ECL spectra were recorded at room temperature using a setup consisting of a F-3010 fluorescence spectrophotometer, CV-27 Voltammograph using Pt wire (0.25 mm diameter, Aldrich), and Pt Gauss (100 mesh (Aldrich), 0.5 cm × 0.5 cm) electrodes together with a Ag/AgCl reference electrode with a computer interface to control the pulsing. The electrode surfaces were prepared freshly before CV and ECL experiments. The carbon disk electrode was rubbed against alumina paste followed by rinsing with double-distilled water and MeCN and wiping with high-quality lint free tissue (Kimberly-Clark delicate wipers). The Pt wire and the Pt Gauss electrodes were cleaned by rinsing with dilute nitric acid followed by water, and then they were finally fired with a naked flame to ensure maximum cleanliness of the electrode. A 1 mM concentration of the compound in dry degassed acetonitrile along with 0.05 M tetrabutylammonium perchlorate (TBAP) and the solution was degassed by purging it with dry argon for both CV and ECL measurements. To generate annihilation reaction for ECL, the platinum electrodes were pulsed between the first reduction and first oxidation potentials and the pulse interval was controlled on a computer. All measurements were done at room temperature (22−23 °C).

Synthesis of 1-Bromopyrene.[20] To a stirred solution of pyrene (2.02 g; 10 mmol) and hydrobromic acid (1.24 mL of a 48% aqueous solution; 11 mmol) in methyl alcohol−ether (20 mL, 1:1) was slowly added hydrogen peroxide (0.34 g; 0.86 mL of a 35% aqueous solution; 10 mmol) over a period of 15 min at 10−15 °C. The reaction was left at room temperature for 12 h while its progress was monitored by TLC. After the completion of monobromination, the solvent was removed under reduced pressure and the crude product was taken in ethyl acetate and washed with water and brine and dried over anhydrous sodium sulfate. The pure product was isolated by careful column chromatography on silica gel to get pure 1-bromopyrene as a light brown solid.

Synthesis of 2-Methyl-4-pyren-1-yl-but-3-yn-2-ol.[21] To a stirred solution of 1-bromopyrene (5.22 mg, 1.86 mmol) and 3-methylbut-1-yn-3-ol (0.38 mL, 3.72 mmol) in piperidine (1 mL) under nitrogen was added $Pd(PPh_3)_4$ (5 mg, 0.0047 mmol), PPh_3 (2 mg, 0.0076 mmol), and a solution of copper iodide (0.014 mmol) and lithium bromide (7.8 mg, 0.09 mmol) in THF (0.5 mL). The clear solution was stirred at 90 °C for 2 h. The reaction mixture was diluted with CH_2Cl_2 and washed with 5% HCl to remove piperidine. The combined organic layer and the solvent were removed under reduced pressure. The crude was pure enough for the next step.

Synthesis of 1-Ethynylpyrene.[21] 2-Methyl-4-pyren-1-yl-but-3-yn-2-ol (800 mg, 2.95 mmol) was suspended in toluene (60 mL) and KOH (1.68 g, 29.5 mmol). Under reflux, the reaction started after 15 min and was complete in 10 min. Finally, 200 mg of KOH was added to the solution to make sure hydration was completed. The pure product was isolated by careful column chromatography on silica gel to get pure 1-ethynylpyrene as a brown solid.

General Procedure for Synthesis of Internal Ethynes (Typical of ANEPy). 9-Bromo-10-cyanoanthracene, palladium catalyst (2 mol %), CuI (2 mol %), triphenylphosphine (10 mol %), and a magnetic stirring bar were placed in a two-necked round-bottom flask fitted with a condenser. The whole setup was degassed and back-filled with a gaseous mixture of argon and hydrogen. To the reaction flask was added previously degassed 5 mL of THF and TEA (10 mmol) using syringes. The terminal acetylene was dissolved in 5 mL of THF and added to the reaction mixture at about 80 °C (bath temperature). The reaction mixture was then stirred at reflux overnight under the atmosphere of the gas mixture. The solvents were evaporated and the crude product was either recrystallized directly or extracted with ether/ethyl acetate (20 mL + 5 × 15 mL). The combined organic layers were washed with water followed by brine before drying and evaporating. The residue after evaporation was chromatographed on silica gel using an ethyl acetate−hexane mixture to separate the products. Following are the characterization data for all compounds:

Dimethyl(4-pyren-1-ylethynylphenyl)amine (DMAEPy). Pale brown crystalline solid. mp: 168−170 °C. ^{1}H NMR (400 MHz, $CDCl_3$): δ 8.67 (d, J = 9.2 Hz, 1H), 8.02−8.18 (m, 8H), 7.59 (d, J = 9.2 Hz, 2H), 6.73 (d, J = 8.4 Hz, 2H), 3.02 (s, 6H). ^{13}C NMR (100 MHz, $CDCl_3$): δ 149.63, 132.405, 131.050, 130.906, 130.761, 130.206, 128.867, 137.535, 127.261, 126.904, 125.717, 125.458, 124.948, 124.887, 124.195, 124.165, 124.073, 118.618, 111.672, 110.013, 96.462, 86.609, 40.518. HRMS (M^+): 345.1517, calcd for $C_{26}H_{19}N$: 345.1517.

1-(4-Isopropoxyphenylethynyl)pyrene (IPPEPy). Yellow solid. mp: 152−155 °C. ^{1}H NMR (400 MHz, $CDCl_3$): δ 8.64 (d, J = 8.8 Hz, 1H), 7.98−8.20 (m, 8H), 7.63 (d, J = 8.4 Hz, 2H), 6.92 (d, J = 8.8 Hz, 2H), 4.60 (m, 1H), 1.38 (d, J = 6.8, 6H). ^{13}C NMR (100 MHz, $CDCl_3$): δ 157.532, 132.743, 131.276, 130.858, 130.698, 130.539, 129.026, 127.749, 127.528, 136.875, 125.795, 125.278, 125.103, 125.058, 124.161, 124.009, 117.981, 115.540, 114.955, 95.191, 87.118, 70.022, 22.405. HRMS (M^+): 360.1512, cacld for $C_{27}H_{20}O$: 360.1514.

1-Phenylethynylpyrene (PhEPy). White crystalline solid. mp: 102−105 °C. ^{1}H NMR (400 MHz, $CDCl_3$): δ 8.65 (d, J = 8.8 Hz, 1H), 7.99−8.22 (m, 8H), 7.72−7.74 (m, 2H), 7.40−7.45 (m, 3H). ^{13}C NMR (100 MHz, $CDCl_3$): δ 131.469, 131.279, 130.822, 130.655, 129.186, 128.091, 128.007, 127.916, 127.733, 126.850, 125.839, 125.230, 125.177, 125.160, 124.149, 124.119, 123.959, 123.183, 117.469, 94.964, 88.542. HRMS (M^+): 302.1019, calcd for $C_{24}H_{14}$: 302.1096.

2-Pyren-1-ylethynylquinoline (2QEPy). Brown crystalline solid. mp: 178−180 °C. ^{1}H NMR (400 MHz, $CDCl_3$): δ 8.77 (d, J = 9.2 Hz, 1H), 8.34 (d, J = 7.6 Hz, 1H) 8.04−8.26 (m, 9H), 7.75−8.02 (m, 3H), 7.58 (t, J = 8.0 Hz, 1H). ^{13}C NMR (100 MHz, $CDCl_3$): δ 147.781, 143.292, 135.653, 132.032, 131.431, 130.677, 130.510, 129.810, 129.643, 128.912, 128.205, 128.174, 127.117, 126.736, 126.713, 126.660, 125.861, 125.466, 125.367, 125.108, 124.195, 124.104, 123.936, 123.746, 116.062, 94.781, 89.280. HRMS (M^+): 353.1191, calcd for $C_{27}H_{15}N$: 353.1204.

10-Pyren-1-ylethynylanthracene-9-carbonitrile (ANEPy). Bright orange crystalline solid. mp: 292−295 °C. ^{1}H NMR (400 MHz, $CDCl_3$): δ 8.94 (dd, 2H), 8.85 (d, J = 8.4 Hz, 1H), 8.50 (dd, 2H), 8.45 (d, 1H), 8.08−8.32 (m, 7H), 8.78 (m, 4H). ^{13}C NMR spectrum could not be recorded due to inadequate solubility. HRMS (M^+): 427.1362, calcd for $C_{33}H_{17}N$: 427.1361.

Theoretical Calculations. Density functional theoretical calculations were performed using Spartan'04(W).[22] Structures were drawn at the entry level of input and minimized. Equilibrium geometry was obtained at the B3LYP level of DFT for each molecule at the ground state from its initial geometry subject to symmetry with the 6-31G* basis set.[23] The total charge was kept neutral or anion/cation as required, and the multiplicity was kept at singlet or doublet as required. Orbitals and energies, atomic charges, vibrational modes, and thermodynamic properties were chosen as output parameters. HOMO and LUMO orbital surfaces and electrostatic potential density maps were then obtained from the output.

Acknowledgment. Financial support for this work was provided by the National Science Council, Taiwan.

Supporting Information Available: ^{1}H NMR, ^{13}C NMR, CV, and raw ECL spectra of all compounds; Cartesian coordinates for all molecules (PDF). This material is available free of charge via the Internet at http://pubs.acs.org.

References and Notes

(1) Nishizawa, S.; Kato, Y.; Teramae, N. *J. Am. Chem. Soc.* **1999**, *121*, 9463.

(2) (a) Tong, A.-J.; Yamauchi, A.; Hayashita, T.; Zhang, Z.-Y.; Smith, R. D.; Termae, N. *Anal. Chem.* **2001**, *73*, 1530. (b) Kim, J. S.; Shon, O. J.; Rim, J. A.; Kim, S. K.; Yoon, J. *J. Org. Chem.* **2002**, *67*, 2348. (c) Corma, A.; Galletero, M. S.; García, H.; Palomares, E.; Rey, F. *Chem. Commun.* **2002**, 1100. (d) Fujiwara, Y.; Okura, I.; Miyashita, T.; Amao, Y. *Anal. Chim. Acta* **2002**, *471*, 25. (e) D'Souza, L. J.; Maitra, U. *J. Org. Chem.* **1996**, *61*, 9494. (f) Sakaki, D. Y.; Padilla, B. E. *Chem. Commun.* **1998**, 1581.

(3) Robers, R. R.; Li, Y.; Lamanski, S. A. U.S. Patent 2004/0214037, Oct 28, 2004.

(4) (a) Rodriguez, J.; Kirmaier, C.; Johnson, M. R.; Friesner, R. A. Holten, D.; Sessler, J. L. *J. Am. Chem. Soc.* **1991**, *113*, 1652. (b) Heiler, D.; McLendon, G.; Rogalskyj, P. *J. Am. Chem. Soc.* **1987**, *109*, 604. Wiessner, A.; Hüttmann, G.; Kühnle, W.; Staerk, H. *J. Phys. Chem.* **1995**, *99*, 14923. (c) Tominaga, K.; Walker, G. C.; Jarzeba, W.; Barbara, P. F. *J. Phys. Chem.* **1991**, *95*, 10475. (d) Rettig, W.; Maus, M.; Lapouyade, R. *Ber. Bunsen-Ges. Phys. Chem.* **1996**, *100*, 2091.

(5) (a) Fiebig, T.; Kühnle, W.; Staerk, H. *Chem. Phys. Lett.* **1998**, *282*, 7. (b) Techert, S.; Schmatz, S.; Wiessner, A.; Staerk, H. *J. Phys. Chem. A* **2000**, *104*, 5700.

(6) (a) Shi, Y.; Zhang, C.; Zhang, H.; Bechtel, J. H.; Dalton, L. R.; Robinson, B. H.; Steier, W. H. *Science* **2000**, *288*, 119. (b) Dalton, L. R.; Steier, W. H.; Robinson, B. H.; Zhang, C.; Ren, A.; Garner, S.; Chen, A.; Londergan, T.; Irwin, L.; Carlson, B.; Fifield, L.; Phelan, G.; Kincaid, C.; Amend, J.; Jen, A. *J. Mater. Chem.* **1999**, *9*, 1905.

(7) (a) Friend, R. H.; Gymer, R. W.; Holmes, A. B.; Burroughes, J. H.; Marks, R. N.; Taliani, C.; Bradley, D. D. C.; Dos Santos, D. A.; Brédas, J.-L.; Lögdlund, M.; Salaneck, W. R. *Nature* **1999**, *397*, 121. (b) Kraft, A.; Grimsdale, A. C.; Holmes, A. B. *Angew. Chem., Int. Ed.* **1998**, *37*, 402.

(8) Brown, A. R.; Pomp, A.; Hart, C. M.; de Leeuw, D. M. *Science* **1995**, *270*, 972.

(9) (a) Yamaguchi, Y.; Kobayashi, S.; Miyamura, S.; Okamoto, Y.; Wakamiya, T.; Matsubura, Y.; Yoshida, Z.-i. *Angew. Chem., Int. Ed.* **2004**, *43*, 366. (b) Boydston, A. J.; Yin, Y.; Pagenkopf, B. L. *J. Am. Chem. Soc.* **2004**, *126*, 3724. (c) Odom, S. A.; Parkin, S. R.; Anthony, J. E. *Org. Lett.* **2003**, *5*, 4245. (d) Pohl, R.; Anzenbacher, P., Jr. *Org. Lett.* **2003**, *5*, 2769. (e) Metivier, R.; Amengual, R.; Leray, I.; Michelet, V.; Genet, J.-P. *Org. Lett.* **2004**, *6*, 739.

(10) (a) Faulkner, L. R., Bard, A. J. Electrogenerated Chemiluminescence. In *Electrochemical Methods*; John Wiley & Sons: New York, 1980; pp 621−627. (b) Faulkner, L. R.; Bard, A. J. *Electroanalytical Chemistry*; Bard, A. J., Ed.; Marcel Dekker: New York, 1977; Vol. 10, pp 1−95. (b) Knight, A. W.; Greenway, G. M. *Analyst* **1994**, *119*, 879. (c) Knight, A. W. *Trends Anal. Chem.* **1999**, *18*, 47. (d) Richter, M. M. *Chem. Rev.* **2004**, *104*, 3003. (e) Lai, R. Y.; Fabrizio, E. F.; Jenekhe, S. A.; Bard, A. J. *J. Am. Chem. Soc.* **2001**, *123*, 9112. (f) Knorr, A.; Daub, J. *Angew. Chem., Int. Ed.* **1995**, *34*, 2664. (g) Prieto, I.; Teetsov, J.; Fox, M. A.; Vanden Bout, D. A.; Bard, A. J. *J. Phys. Chem. A* **2001**, *105*, 520. (h) Oyama, M.; Okazaki, S. *Anal. Chem.* **1998**, *70*, 5079. (i) Kapturkievicz, A. *J. Electroanal. Chem.* **1990**, *290*, 135. (j) Kapturkievicz, A. *J. Electroanal. Chem.* **1991**, *302*, 13. (k) Faulkner, L. R.; Tachikawa, H.; Bard, A. J. *J. Am. Chem. Soc.* **1972**, *94*, 691.

(11) Faulkner, L. R.; Bard, A. J. *Electroanalytical Chemistry*; Bard, A. J., Ed.; Marcel Dekker: New York, 1977; Vol. 10, pp 1−95.

(12) Turro, N. J. *Modern Molecular Photochemistry*; The Benjamin/Cummings Publishing Co., Inc.: Menlo Park, CA, 1978.

(13) (a) Anderson, J. D.; McDonald, E. M.; Lee, P. A.; Anderson, M. L.; Ritchie, E. L.; Hall, H. K.; Hopkins, T.; Mash, E. A.; Wang, J.; Padias, A.; Thayumanavan, S.; Barlow, S.; Marder, S. R.; Jabbour, G. E.; Shaheen, S.; Kippelen, B.; Peyghambarian, N.; Wightman, R. M.; Armstrong, N. R. *J. Am. Chem. Soc.* **1998**, *120*, 9646. (b) Armstrong, N. R.; Anderson, J. D.; Lee, P. A.; McDonald, E. M.; Wightman, R. M.; Hall, H. K.; Hopkins, T.; Padias, A.; Thayumanavan, S.; Barlow, S.; Marder, S. R. *SPIE* **1999**, *3476*, 178. (c) Armstrong, N. R.; Whightman, R. M.; Gross, E. M. *Annu. Rev. Phys. Chem.* **2001**, *52*, 391.

(14) (a) Wang, S.-L.; Ho, T.-I. *J. Photochem. Photobiol., A: Chem.* **2000**, *135*, 119. (b) Chen, F.-C.; Ho, J.-H.; Chen, C.-Y.; Su, Y. O.; Ho, T.-I. *J. Electroanal. Chem.* **2001**, *499*, 17.

(15) Reynolds, G. A.; Drexhage, K. H. *Opt. Commun.* **1975**, *13*, 222.

(16) (a) Lakovickz, J. R. *Principles of Fluorescence Spectroscopy*; Plenum Press: New York, 1983; p 187. (b) Lippert, Von E. *Z. Electrochem.* **1957**, *61*, 962.

(17) Harriman, A.; Hissler, M.; Ziessel, R. *Phys. Chem. Chem. Phys.* **1999**, *1*, 4203.

(18) (a) Chen, F.-C.; Ho, J.-H.; Chen, C.-Y.; Su, Y. O.; Ho, T.-I. *J. Electroanal. Chem.* **2001**, *499*, 17. (b) Elangovan, A.; Chen, T.-Y.; Chen, C.-Y.; Ho, T.-I. *Chem. Commun.* **2003**, 2146.

(19) (a) Elangovan, A.; Yang, S.-W.; Lin, J.-H.; Kao, K.-M.; Ho, T.-I. *Org. Biomol. Chem.* **2004**, *2*, 1597. (b) Elangovan, A.; Chiu, H.-H.; Yang, S.-W.; Ho, T.-I. *Org. Biomol. Chem.* **2004**, *2*, 3113. (c) Ho, T.-I.; Elangovan, A.; Hsu, H.-Y.; Yang, S.-W. *J. Phys. Chem. B* **2005**, *109*, 8626. (d) Elangovan, A.; Lin, J.-H.; Yang, S.-W.; Hsu, H.-Y.; Ho, T.-I. *J. Org. Chem.* **2004**, *69*, 8086. (e) Elangovan, A.; Kao, K.-M.; Yang, S.-W.; Chen, Y.-L.; Ho, T.-I.; Su, O. Y. *J. Org. Chem.* **2005**, *70*, 4464.

(20) Vyas, P. V.; Bhatt, A. K.; Ramachandraiah, G.; Bedekar, A. V. *Tetrahedron Lett.* **2003**, *44*, 4085.

(21) Crip, G. T.; Jiang, Y.-L. *Synth. Commun.* **1998**, *28*, 2571.

(22) *Spartan'04 Windows*; Wavefunction, Inc.: Irvine, CA.

(23) (a) Hehre, W. J. *A Guide to Molecular Mechanics and Quantum Chemical Calculations*; Wavefunction, Inc.: Irvine, 2003. (b) Lee, C.; Yang, W.; Parr, R. G. *Phys. Rev. B* **1988**, *37*, 785. (c) Becke, A. D. *J. Chem. Phys.* **1993**, *98*, 5648.

(24) Kamlet, M. K.; Abbound, J. L. M.; Abraham, M. H.; Taft, R. W. *J. Org. Chem.* **1983**, *48*, 2877.

(25) Maloy, J. T.; Bard, A. J. *J. Am. Chem. Soc.* **1971**, *93*, 5968.